



## Relationships between development of organic-rich shallow shelf facies and variation in isotopic composition of pyrite (Middle Triassic, Spitsbergen)

Przemysław KARCZ

*Państwowy Instytut Geologiczny – Państwowy Instytut Badawczy,  
Rakowiecka 4, 00-975 Warszawa, Poland  
<przemyslaw.karcz@pgi.gov.pl>*

**Abstract:** 51 samples from the Middle Triassic black shales (organic carbon-rich siltstones; up to 4.9% TOC – Total Organic Carbon) from the stratotype section of the Bravaisberget Formation (western Spitsbergen) were analyzed with respect to isotopic composition of pyritic sulphur ( $\delta^{34}\text{S}$ ) and TOC. Isotopic composition of syngenetic pyrite-bound sulphur shows wide ( $\delta^{34}\text{S}$  from  $-26\text{‰}$  to  $+8\text{‰}$  VCDT) and narrow ( $\delta^{34}\text{S}$  from  $-4\text{‰}$  to  $+17\text{‰}$  VCDT) variation of the  $\delta^{34}\text{S}$  in upper and lower part of the section, respectively. Range of the variation is associated with abrupt changes in dominant lithology. Wide  $\delta^{34}\text{S}$  variation is found in lithological intervals characterized by alternation of black shales and phosphorite-bearing sandstones. The narrow  $\delta^{34}\text{S}$  variation is associated with the lithological interval dominated by black shales only. Wide and narrow variation of the  $\delta^{34}\text{S}$  values suggests interplay of various factors in sedimentary environment. These factors include oxygen concentration, clastic sedimentation rate, bottom currents and burrowing activity. Biological productivity and rate of dissimilatory sulphate reduction had important impact on the  $\delta^{34}\text{S}$  variation as well. Wide variation of the  $\delta^{34}\text{S}$  values in the studied section resulted from high biological productivity and high rate of dissimilatory sulphate reduction. Variable degree of clastic sedimentation rate and burrowing activity as well as the activity of poorly oxygenated bottom currents could also cause a co-occurrence of isotopically light and heavy pyrite in differentiated diagenetic micro-environments. Occurrence of organic matter depleted in hydrogen could also result in a wide variation of the  $\delta^{34}\text{S}$  values. Narrow variation of the  $\delta^{34}\text{S}$  values was due to a decrease of biological productivity and low rate of dissimilatory sulphate reduction. Low organic matter supply, low oxygen concentration and bottom currents and burrowing activity were also responsible for narrow variation of the  $\delta^{34}\text{S}$ . The narrow range of the  $\delta^{34}\text{S}$  variation was also due to occurrence of hydrogen-rich organic matter. In the studied section the major change in range of the  $\delta^{34}\text{S}$  variation from wide to narrow appears to be abrupt and clearly associated with change in lithology. The change of lithology and isotopic values may suggest evolution of the sedimentary environment from high- to low-energy and also facies succession from shallow to deeper shelf. The evolution should be linked with the Late Anisian regional transgressive pulse in the Boreal Ocean.

Key words: Arctic, Svalbard, Bravaisberget Formation, sulphur isotopes, organic carbon.

## Introduction

Lower and Middle Triassic organic-rich deposits of Svalbard and adjacent Barents Sea Shelf areas have been classified as the Sassendalen Group (Buchan *et al.* 1965; Mørk *et al.* 1982). On the Svalbard archipelago, the Sassendalen Group is exposed on Spitsbergen, Barentsøya and Edgeøya and in southern and western parts of Nordaustlandet (Fig. 1). The group is dominated by clastic deposits, *i.e.* shales and



Fig. 1. Sketch map of the Svalbard archipelago showing outcrops of the Sassendalen Group (after Dallmann 1999) and the distribution of the Bravaisberget and Botneheia formations. VK-Van Keulenfjorden.

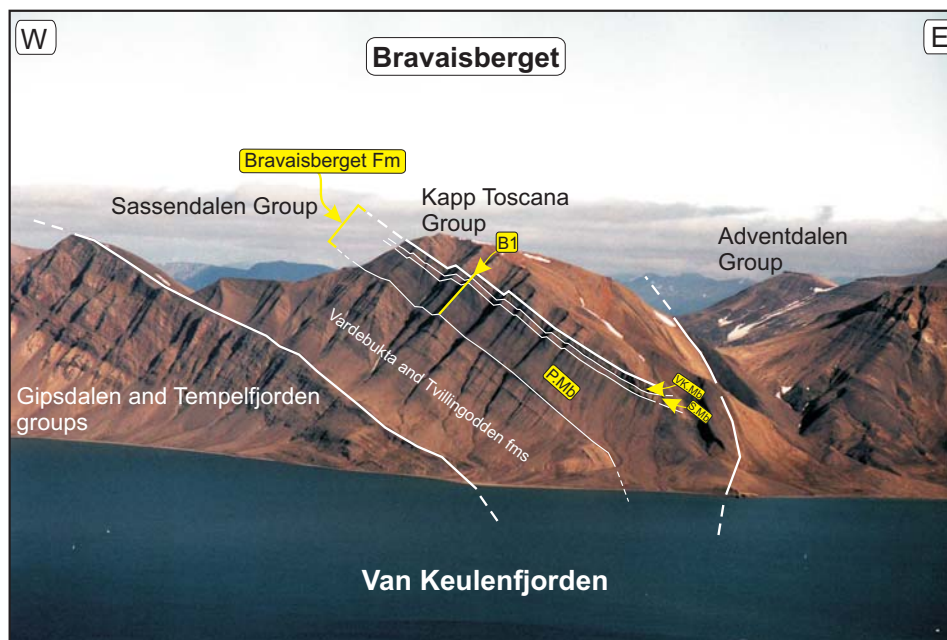


Fig. 2. A scenic picture of the south-western slope of Bravaisberget exposed towards Van Keulenfjorden. White thick lines mark a group boundaries, whilst white thin lines mark formation and member boundaries. The analyzed profile of the Bravaisberget Fm is marked as B1. Detailed information about type section of the Bravaisberget Fm was published in Krajewski *et al.* (2007). P.Mb – Passhatten Mb; S.Mb – Somovbreen Mb; VK.Mb – Van Keulenfjorden Mb. Photograph by K.P. Krajewski.

siltstones with subordinate sandstones and carbonate rocks. The Sassendalen Group contains several transgressive-regressive cycles (Mørk *et al.* 1982, 1989, 1999).

Several formations have been distinguished in the group. One of them is the Bravaisberget Fm (Mørk *et al.* 1982), comprising the most westward exposed Middle Triassic sedimentary sequence on Svalbard. The formation is stretching along western Spitsbergen (Fig. 1). Thickness of the Bravaisberget Fm in western Nathorst Land exceeds slightly 200 m (Fig. 2).

The formation consists of black shales interspaced by siltstones with fine-grained sandstones. The black shales are organic carbon-rich siltstones deposited in shallow shelf environment. The recorded TOC values range from 0.6 to 4.9 wt.% (Karcz 2008, 2009).

The Bravaisberget Fm is Anisian-Ladinian in age (Buchan *et al.* 1965; Mørk *et al.* 1982).

The Bravaisberget Fm in its stratotype location has been subdivided into three members: (1) the Passhatten Mb, (2) the Somovbreen Mb, and (3) the Van Keulenfjorden Mb (Mørk *et al.* 1999, Krajewski *et al.* 2007). The Passhatten Mb (Birkenmajer 1977) (about 160 meters thick) embraces lower and middle parts of the formation and is represented by black shale beds intercalated with phospho-

rite-bearing sandstones. The black shales were deposited on the muddy bottoms under conditions of oxygen deficiency and intense reworking of sediments by bottom currents. On the other hand, phosphorite-rich sandstones reflect progradation of the shallow sandy facies, accompanied by sediment redeposition and its gravity transport along and across the clastic bars (Krajewski *et al.* 2007). Recurrent occurrences of black shales and phosphorite-bearing sandstones in the section are indicative of low energy sea bottom environment with low oxygen content, and much better oxygenated environment, respectively (Mørk and Bjorøy 1984; Krajewski *et al.* 2007; Mørk and Bromley 2008).

In the Anisian and Ladinian, the Passhatten Mb sediments were accumulated in the shallow shelf environment. To the west and southwest of the present-day Spitsbergen coastline, the depositional environment was bordered by land area with well developed delta systems (Mørk *et al.* 1982; Mørk and Bjorøy 1984; Krajewski 2000; Riss *et al.* 2008; Mørk and Bromley 2008).

Within the Passhatten Mb section, two transgressive pulses have been recognized. The first one, Early Anisian in age, marks a boundary of the member with the underlying Tvillingodden Fm which is Olenekian in age (Mørk *et al.* 1982). Based on sequence stratigraphy Mørk *et al.* (1989) consider that the second transgressive pulse took place in the Late Anisian. The two transgressive pulses are probably responsible for decrease of dynamics of the basin and bottom environment.

According to Mørk *et al.* (1982); Steel and Worsley (1984) and Krajewski (2000), well developed upwelling currents system, nutrients supply from adjacent land areas and transgressive pulses were responsible for the increase of biological productivity in the Triassic shelf environment of Svalbard.

The Passhatten Mb section has been additionally subdivided into two parts, the lower and the upper. The parts are associated with Early and Late Anisian transgressive pulses, respectively. The subdivision has been introduced on the basis of the recorded differences in geochemical and petrographical features (Karcz 2008, 2009):

- 1) The lower part – deposited after Early Anisian transgressive pulse. It is characterized by wide variation of the DOP (Degree of Pyritization),  $\delta^{34}\text{S}$ , TOC and reactive iron values.
- 2) The upper part – deposited after Late Anisian transgressive pulse and characterized by narrow variation of the above mentioned geochemical indicators (Karcz 2008).

The parts of the Passhatten Mb correspond to lithological intervals between sampling points B1–12 and B1–104, and B1–106 and B1–146, respectively (Fig. 3).

Boundary between these two parts has been traced in very short lithological section of the Passhatten Mb confined to the lithological interval between the sampling points B1–104 and B1–106 (Fig. 3). The subdivision is further supported by a higher content of fine-grained clastics in the upper part than in the lower one (Krajewski *et al.* 2007; Karcz 2008).

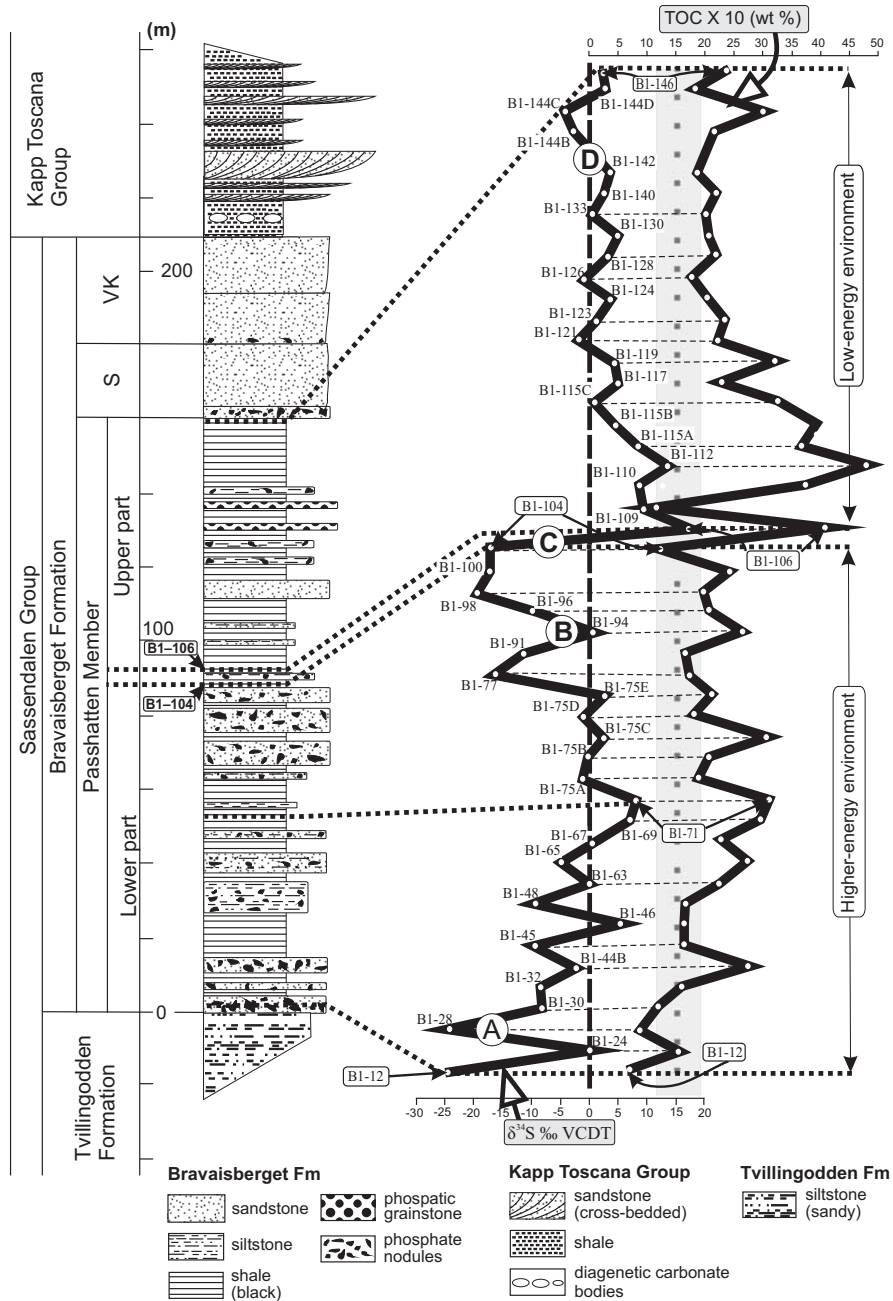


Fig. 3. Simplified section of the stratotype of the Bravaisberget Fm against the plot of isotopic composition of pyritic sulphur ( $\delta^{34}\text{S}$ , ‰ VCDT) and organic carbon content (TOC, wt%). Profile after Krajewski *et al.* (2007). A, B, C and D – parts of the isotopic curve (detailed explanation in text). B1-12, 71, 104, 106 and 146 – sampling points mark the boundaries between lithological intervals with different isotopic trends. Vertical dotted line with grey adjacent field is an average value of  $\delta^{34}\text{S}$  of Triassic sea water sulphate (Fanlo and Ayora 1998). S – Somvreen Mb; VK – Van Keulenfjorden Mb.

## Samples

Geochemical and microscopic analysis was carried out only on black shale samples. The samples were collected from the stratotype section of the Bravaisberget Fm located in the western Nathorst Land at Bravaisberget (Fig. 2) by K.P. Krajewski and B. Luks during the expedition of the Polish Academy of Sciences to Svalbard in 2002. The section has been sampled along the rocky rib marked as B1 (Fig. 2; Krajewski *et al.* 2007). Thickness of the formation along the B1 section is 210 meters.

The black shales cover a spectrum from silty shales, through sandy siltstones to muddy and silty sandstones (Krajewski *et al.* 2007; Karcz 2008). Sedimentary features of the black shales vary between individual lithological intervals, from small scale cross-laminated in the lower part to planar-laminated internal structure in the upper part. The planar-laminated internal structure is often accentuated by directional arrangement of calcified fragments of thin-shelled pelecypods (Karcz 2008).

The main mineral constituent of the examined sedimentary rocks is quartz. Average content of quartz is about 23% in silty shales and sandy siltstones, increasing up to 50% in silty sandstones.

The minerals occurring here as subordinate rock components include muscovite, biotite and chlorite (1–5%). Detrital feldspar and heavy minerals as titanite, rutile, tourmaline, zircon and garnet are here accessory.

Bioturbations are abundant in all the studied petrographic rock types. Vertical and horizontal bioturbations are from about 2 to 10 mm in size. Statistic analysis of bioturbations revealed that the structures are more common in the black shales from the lower part than the upper (Karcz 2008).

Early-diagenetic pyrite (formed as a result of dissimilatory sulphate reduction) occurs as an accessory mineral in all analyzed rock samples as single dispersed or concentrated microcrystals and/or (poly)framboids. Microcrystals dominate over (poly)framboids in the entire analyzed section. Content of the latter decreases significantly in the upper part (Karcz 2008, 2009).

## Methods

Black shale samples were crushed to provide very fine rock fragments and subsequently dried and powdered using an agate mortar and pestle. Elemental sulphur and acid volatile sulphides were extracted by treating the samples with acetone and with 6N HCl in the presence of  $\text{SnCl}_2 \cdot 2\text{H}_2\text{O}$ . The process was carried out in nitrogen atmosphere for 15 minutes. The samples were boiled for 5 minutes. In the studied samples neither presence of acid volatile sulphides nor elemental sulphur was detected; therefore methodology recommended by Canfield *et al.* (1986) and Zaback and Pratt (1992) was applied.  $\text{H}_2\text{S}$  was obtained from pyrite decomposition

by treating the residuum with 12 N HCl and 1 M CrCl<sub>2</sub> in nitrogen atmosphere (for details see Canfield *et al.* 1986). H<sub>2</sub>S precipitated as Ag<sub>2</sub>S by reacting with 5% AgNO<sub>3</sub>. SO<sub>2</sub> for spectrometric measurements was obtained by thermal decomposition of Ag<sub>2</sub>S with CuO at 1000°C in vacuum line and purified by cryogenic distillation (the methods were described in detail in Fritz *et al.* 1974). Isotopic <sup>34</sup>S/<sup>32</sup>S ratios were determined using a Finnigan Mat Delta<sup>plus</sup> spectrometer at the Institute of Geological Sciences of the Polish Academy of Sciences in Warszawa. The results are given as δ<sup>34</sup>S deviation relative to Cañon Diablo Troilite (VCDT) standard. The δ<sup>34</sup>S values are reproducible to ± 0.10‰.

Rock Eval results are given in Table 1. The Rock Eval analysis have been carried out on washed pulverized samples. 100 mg of each black shale sample was analyzed using a Rock Eval 6 instrument. The pyrolysis technique was outlined in detail by Espitalié *et al.* (1985). Parameter S1 is a measure of amount of hydrocarbons liberated at 300°C. Parameter S2 is amount of hydrocarbons released during temperature-programmed pyrolysis (300–600°C). TOC is determined by oxidizing the pyrolysis residue in the second oven. Hydrogen index (HI) is the normalized S2 value (S2/TOC) expressed as mg HC/g TOC, which facilitates identification of types of organic matter. Rock Eval analysis has been carried out at the Institute of Oil and Gas in Kraków.

## Results

The obtained sulphur isotopic values of pyritic sulphur are given in Table 1. The δ<sup>34</sup>S values fall in the range between 26‰ and +17‰ VCDT. In the lowermost lithological interval of the Passhatten Mb (between sampling points B1–12 and B1–71) δ<sup>34</sup>S values show wide variation ranging from -26‰ to +8‰ VCDT (Fig. 3). In the upper interval of the Passhatten Mb (between sampling points B1–75A and B1–104) δ<sup>34</sup>S values fall within more narrow range between -20‰ and +2‰ VCDT. Very short interval between sampling points B1–104 and B1–106 shows very wide variation of the δ<sup>34</sup>S values from -17‰ (B1–104) to +17‰ VCDT (B1–106) (Table 1 and Fig. 3). The uppermost interval of the Passhatten Mb (between sampling points B1–106 and B1–146) is characterized by δ<sup>34</sup>S values between -4‰ and +17‰ VCDT.

The total organic carbon values fall in the range between 0.6 and 4.9 weight% (Table 1 and Fig. 3). The lower part of the Passhatten Mb is characterized by lower average TOC value 2%, whilst in the upper part the value increases up to 2.5%.

HI values fall in the range between 55 and 122 mg HC/g TOC (Table 1). The lower part is characterized by wide variation of the HI values from 55 to 122 mg HC/g TOC. The upper part shows narrower HI variation, from 71 to 114 mg HC/g TOC. Average values for the lower and upper parts are 91 and 102 mg HC/g TOC, respectively.

Table 1  
 Results data for TOC (weight%), HI (mg HC/g TOC) and  $\delta^{34}\text{S}$  (‰; VCDT) for black shales  
 of the Passhatten Mb.

Samples	TOC (weight %)	HI (mg HC/g TOC)	Isotopic composition of pyrite ( $\delta^{34}\text{S}$ , ‰ VCDT)
B1-146	2.4	114	1.9
B1-144 D	1.9	99	2.6
B1-144 C	3.1	106	-4.7
B1-144 B	2.2	102	-3.4
B1-142	1.9	90	-3.3
B1-140	2.2	100	2.1
B1-133	2.0	107	-0.1
B1-130	2.1	107	4.7
B1-128	2.2	98	2.6
B1-126	1.8	71	-1.3
B1-124	2.1	100	3.6
B1-123	2.4	93	0.7
B1-121	2.2	100	-2.6
B1-119	3.3	105	4.1
B1-117	2.3	102	4.7
B1-115 C	3.3	112	0.4
B1-115 B	4.0	109	4.2
B1-115 A	3.7	113	8.0
B1-112	4.9	109	13.6
B1-110	3.8	105	8.5
B1-109	1.1	94	9.2
B1-106	2.9	110	17.6
B1-104	1.2	113	-17.9
B1-100	2.5	89	-18.3
B1-98	2.0	98	-20.3
B1-96	2.1	98	-9.6
B1-94	2.7	94	0.5
B1-91	1.7	89	-12.4
B1-77	1.7	95	-17.4
B1-75 E	2.2	100	2.3
B1-75 D	1.8	87	-1.3
B1-75 C	3.2	113	2.2
B1-75 B	2.1	93	-0.6
B1-75 A	1.9	98	-1.6
B1-71	3.2	106	8.2
B1-69	3.0	86	6.8
B1-67	2.3	106	1.0
B1-65	2.8	120	-5.5
B1-63	2.3	104	-0.1
B1-48	1.7	78	-10.4
B1-46	1.8	55	5.4
B1-45	1.7	77	-10.4
B1-44 B	2.8	78	-2.8
B1-32	1.6	99	-9.0
B1-30	1.2	83	-9.0
B1-28	0.9	63	-25.8
B1-24	1.6	82	0.1
B1-12	0.7	95	-26.1

## Discussion

Wide and narrow variation in isotopic composition of pyritic sulphur was due to two-stage development of the Passhatten Mb. Wide variation was coupled with recurrent deposition of the different lithological intervals *i.e.* black shales and phosphorite-bearing sandstones classified in this paper as lower part of the Passhatten Mb. Whereas narrow variation in isotopic composition was coupled with more monotonous deposition of the black shales lithological interval presented here as upper part of the Passhatten Mb. The two-stage development of the Passhatten Mb is also reflected by a transition from high to low energy sedimentary environment. The first and second stage of deposition of the sediments occurred after Early and Late Anisian transgressive pulses, respectively. Both transgressive pulses had a major influence on factors controlling  $\delta^{34}\text{S}$  variation in the sedimentary environment. Those factors included: clastic sedimentation rate, rate of burial of organic matter and its exposition to oxygenated bottom currents and burrowing organisms.

Trend towards heavier values in isotopic composition of pyritic sulphur occurs within the lithological intervals between sampling points B1–12 and B1–71 (part A of isotopic curve) and B1–104 and B1–106 (part C the curve) (Fig. 3). This trend in isotope values is interpreted as associated with change of oxygen concentration in the bottom environment *i.e.* with gradual and rapid decreasing of degree of oxygenation, respectively. Then, trend towards heavier values should be interpreted as a result of increased anoxicity. Relationship between positive  $\delta^{34}\text{S}$  values in authigenic pyrite and increase of the degree of anoxicity have been also evidenced in other diagenetic environments by Habicht and Canfield (1997), Lyons (1997), Brüchert (1998), Hurtgen *et al.* (1999), Brüchert *et al.* (2000).

Another process favorable for development of trend towards heavier values in isotopic composition of pyritic sulphur is the increase of sedimentation rate. Probably the gradual increase of the rate of sedimentation took place during deposition of the lithological interval between sampling points B1–12 and B1–71. It correlates well with gradual increase in share of  $^{34}\text{S}$ -enriched pyrite (part A of isotopic curve; Fig. 3). It may suggest that increased clastic material supply caused isolation of authigenic pyrite from oxidants. The argument have been also evidenced by Gautier (1987); Lyons (1997); Aharon and Fu (2000); Jørgensen *et al.* (2004); Neretin *et al.* (2004) in other diagenetic environments.

Trend towards lighter values in isotopic composition of pyritic sulphur is found in the lithological intervals between sampling points B1–71 and B1–104, and B1–106 and B1–146 (Fig. 3). This trend was associated with gradual increase of oxygen concentration in the bottom environment (part B of the isotopic curve, Fig. 3). On the other hand, enhanced degree of oxygenation probably resulted from higher contribution of oxygenated bottom currents and higher energy in this sedi-

mentary environment. Relationship between trend towards lighter values in isotopic composition of pyritic sulphur and increased oxygen concentration have been well evidenced by Böttcher *et al.* (2001); Böttcher and Thamdrup (2001); Werne *et al.* (2003).

A higher energy shallow shelf sedimentary environment is characterized by co-occurrence of oxic, dysoxic and anoxic bottom currents, which may lead to recurrent oxidation and reduction processes. If this was the case, isotopically light sulphides could be the result of H<sub>2</sub>S oxidation and disproportionation (Canfield and Thamdrup 1994; Werne *et al.* 2003). The process probably occurred during deposition of the lithological interval linked with part B of the isotopic curve.

Formation of the isotopically light sulphides was also controlled by oxidation and reduction rate. Low oxidation and reduction rate with contribution of sulphur intermediate compounds (S<sub>2</sub>O<sub>3</sub><sup>2-</sup> and SO<sub>3</sub><sup>2-</sup>) could lead to formation of isotopically light sulphides (Jørgensen 1990; Habicht *et al.* 1998; Böttcher *et al.* 2001; Leśniak *et al.* 2003). The process could occur in the uppermost part of the studied interval of the Passhatten Mb (between sampling points B1–106 and B1–146), which is dominated by black shales. Usually, such lithological horizons are considered to be the result of deposition under low-energy conditions in stratified basins, whereas bioturbations and other indices of oxygenation occurring in the interval, show periodically broken stratification and more or less normal oxygen access to the sea bottom environment.

Wide variation in isotopic composition of pyritic sulphur ( $\delta^{34}\text{S}$ ) in the lower part of the Passhatten Mb (Fig. 3), resulted from high rate of dissimilatory sulphate reduction. The process was probably due to high biological productivity conditions widespread in the Middle Triassic surficial waters of Svalbard shelf. Relationship between wide variation of the  $\delta^{34}\text{S}$  pyritic sulphur and high organic matter supply have been found in many sedimentary environments (Aharon and Fu 2000; Jørgensen *et al.* 2001; Weber *et al.* 2001; Brüchert *et al.* 2003).

Variable rates of clastic sedimentation and changes in activity of anoxic, dysoxic and oxic bottom currents were most probably responsible for redoxcline fluctuations in the bottom environment. The processes led to co-occurrence of the isotopically heavy and light pyrite, which is recorded in lower part of the Passhatten Mb. The microscopic studies showed small cross-, ripple-, bioturbated as well as planar-laminated and non-bioturbated recurrent beds, that is the sedimentary environment favorable for wide variation of the  $\delta^{34}\text{S}$  (Fig. 3).

The range of the  $\delta^{34}\text{S}$  variation was also controlled by the type of organic matter. Wide and narrow variation in isotopic composition of pyritic sulphur was due to occurrence of hydrogen-depleted and hydrogen-rich organic matter, respectively (Figs 4, 5). Then, parts A and B of the isotopic curve show presence of hydrogen-depleted organic matter (Fig. 3). This suggests that organic matter settling

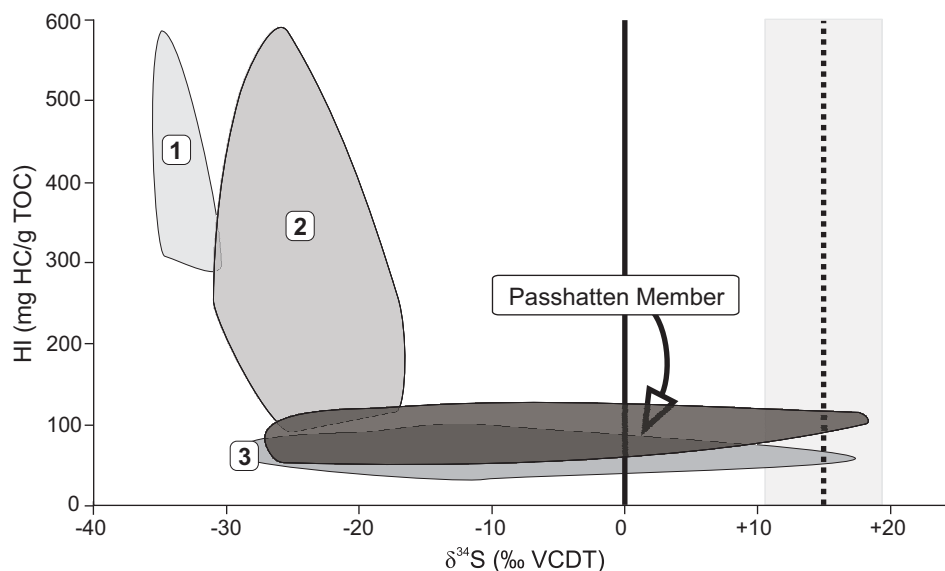


Fig. 4. Relationship between hydrogen index (HI) and isotopic composition of pyritic sulphur ( $\delta^{34}\text{S}$ ; ‰ VCDT) for black shales of the Passhatten Mb and for black shales of the various origin and age. 1 – black shales of the Sharon Springs Mb; 2 – black shales of the Greenhorn Fm; 3 – Gammon black shales. Data for 1, 2 and 3 are based on Gautier (1987). Vertical dotted line with grey adjacent field is an average value of  $\delta^{34}\text{S}$  of Triassic sea water sulphate (Fanlo and Ayora 1998).

on the sea bottom has been reworked by oxic and dysoxic bottom currents. This also suggests a higher energy of the environment.

Gautier (1987) considers wide isotopic variation of the pyritic sulphur to be also a result of pyrite precipitation within differentiated micro-environments of the sea bottom. Such micro-environments are related to a high energy environment, variable rate of clastic sedimentation and increase in activity of currents and burrowing organisms. Activity of the organisms could cause an injection and mixing of less and more decomposed organic matter into burrow structures. Therefore, varied reactivity of organic matter predisposed wide variation in isotopic composition of pyritic sulphur. The process occurred during deposition of the lower part of the Passhatten Mb.

Narrow variation in the isotopic composition of pyritic sulphur ( $\delta^{34}\text{S}$ ) discerned in the upper part of the Passhatten Mb (Fig. 3, part D of isotopic curve) resulted from low rate of dissimilatory sulphate reduction. The process was probably a consequence of the decreased biological productivity in the Middle Triassic shelf environment of western Spitsbergen. The latter process presumably has been caused by migration of primary producers, resulting from Late Anisian transgressive pulse. The pulse is traceable in the lithological interval between sampling points B1–104 and B1–106 and well correlates with the part C of the isotopic curve (Fig. 3). That transgressive event changed the Middle Triassic

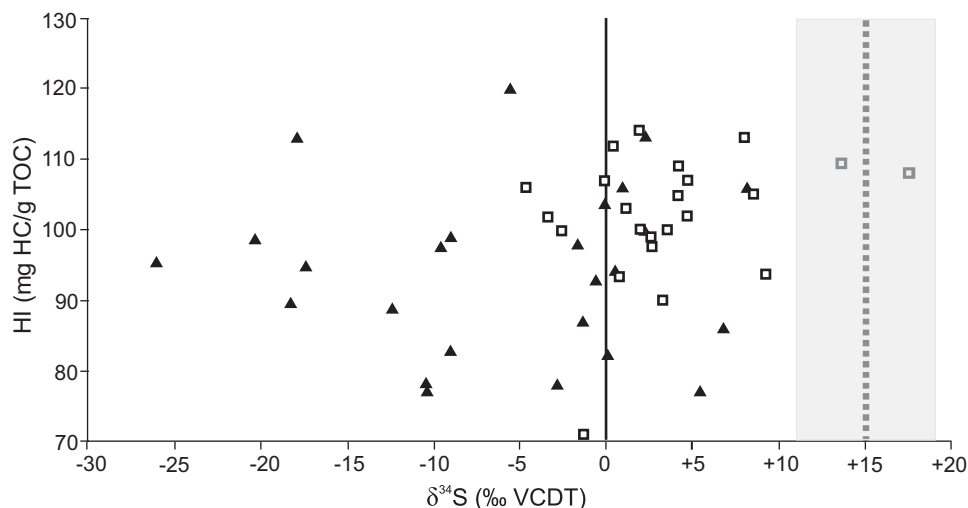


Fig. 5. Relationship between hydrogen index (HI) and isotopic composition of pyritic sulphur ( $\delta^{34}\text{S}$ ; ‰ VCDT) for black shales of the Passhatten Mb.  $\blacktriangle$  – samples from lower part of the profile;  $\blacksquare$  – samples from upper part of the profile. Vertical dotted line with grey adjacent field is an average value of  $\delta^{34}\text{S}$  of Triassic sea water sulphate (Fanlo and Ayora 1998).

shallow shelf sedimentary environment of western Spitsbergen from high-energy to more stagnant, low-energy. The change led to a decrease in sedimentation rate and concentration of oxygen in bottom environment. Increase of water column depth contributed to widespread stratification and anoxicity in the sedimentary environment. Those factors were largely favorable to monotonous deposition of the black shale sequences and development of homogeneity of the diagenetic environment. The lithological interval between sampling points B1–106 and B1–146 is almost devoid of bioturbations and characterized by small share of very fine and silty sandstone intercalations. Therefore, that interval may be best interpreted as representing sedimentary environment favorable for deposition of reactive and hydrogen-rich organic matter. This explains why isotopic composition of pyritic sulphur ( $\delta^{34}\text{S}$ ) in that part of the section is characterized by narrow range of variation (Fig. 5).

Isotopic composition of pyritic sulphur ( $\delta^{34}\text{S}$ ) was also affected by organic matter content and correlation between the two factors was found to be positive (Fig. 3). Decreases and increases in content of organic matter coincide with the presence of  $^{34}\text{S}$ -depleted and  $^{34}\text{S}$ -enriched pyrite, respectively. This relationship is observed in the whole section of the Passhatten Mb. This suggests that organic matter deposited in the black shales was fresh and reactive. Immediately after deposition, the organic matter was decomposed by microbial communities. Enhanced supply of organic matter was coupled with its accelerated decomposition by microbial communities as well as with spreading of anoxia. Therefore, high reactivity of the organic matter should be the evidence of its autochthonous origin.

## Conclusions

The isotopic composition of pyritic sulphur in the Middle Triassic black shales in western Spitsbergen shows wide and narrow  $\delta^{34}\text{S}$  variation in authigenic pyrite, reflecting changes in sedimentary environment. These changes were enforced by the scale of biological productivity, rate of dissimilatory sulphate reduction, degree of oxygenation of bottom water, rate of clastic sedimentation and activity of bottom currents and burrowing communities.

Wide variation of the  $\delta^{34}\text{S}$  values in the lower part of the Passhatten Mb was due to high biological productivity in the Middle Triassic depositional system of Svalbard. Enhanced organic matter production in the surficial waters and its supply to the sea bottom has caused enhanced decomposition of the settled organic matter by microbial communities. Rate of dissimilatory sulphate reduction was high as a result of the high supply of reactive organic matter. The process has caused wide variation of the  $\delta^{34}\text{S}$  values. Variable rate of clastic sedimentation, burrowers activity and activity of well and poorly oxygenated bottom currents could also lead to a co-occurrence of isotopically light and heavy pyrite in those highly diversified diagenetic micro-environments. Also presence of organic matter of lower reactivity contributed to wide variation of the  $\delta^{34}\text{S}$  values.

Narrow variation of the  $\delta^{34}\text{S}$  values in the upper part of the member was probably related to a decrease in biological productivity and rate of dissimilatory sulphate reduction as a consequence of decrease of population of primary producers. That population most probably migrated after the Late Anisian transgressive pulse, which led to deepening of the sedimentary environment. The change of the environment from high- to low-energy in the area of the Bravaisberget locality has caused decrease in supply of organic matter and activity of bottom currents and burrowing communities. It should be added that the evolution also contributed to extension of conditions favorable for preservation of hydrogen-rich organic matter.

Evolution of the sedimentary environment after Late Anisian transgressive pulse has caused that black shales of the upper part of the Passhatten Mb are much better quality source rock for hydrocarbon generation than rocks from lower part (publication in preparation).

**Acknowledgements.** — The article presents the results of PhD dissertation (Karcz 2008). The dissertation has been carried out under scientific supervision of Associate Professor Krzysztof P. Krajewski at the Institute of Geological Sciences, Polish Academy of Sciences. I am grateful to Krzysztof P. Krajewski, Paweł M. Leśniak, Atle Mørk and Tadeusz Peryt for helpful suggestions, constructive comments and review of first draft of this manuscript. I appreciate the laboratory assistance of Bożena Łącka and Paweł Zawidzki during samples preparation and isotopic measurements. Irena Matyasik is greatly acknowledged for Rock Eval analysis.

## References

- AHARON P. and FU B. 2000. Microbial sulfate reduction rates and sulphur and oxygen isotope fractionation at oil and gas seeps in deep water Gulf of Mexico. *Geochimica Cosmochimica Acta* 64: 233–246.
- BIRKENMAJER K. 1977. Triassic sedimentary formations of the Horsund area, Spitsbergen. *Studia Geologica Polonica* 51: 7–74.
- BÖTTCHER M.E. and THAMDRUP B. 2001. Anaerobic sulfide oxidation and stable isotope fractionation associated with bacterial sulphur disproportionation in the presence of MnO<sub>2</sub>. *Geochimica Cosmochimica Acta* 65: 1573–1581.
- BÖTTCHER M.E., THAMDRUP B. and VENNEMANN T.W. 2001. Oxygen and sulphur isotope fractionation during anaerobic bacterial disproportionation of elemental sulphur. *Geochimica Cosmochimica Acta* 65: 1601–1609.
- BRÜCHERT V. 1998. Early diagenesis of sulphur in estuarine sediments: The role of sedimentary humic and fulvic acids. *Geochimica Cosmochimica Acta* 62: 1567–1586.
- BRÜCHERT V., PEREZ M.E. and LANGE C.B. 2000. Coupled primary production, benthic foraminiferal assemblage, and sulphur diagenesis in organic-rich sediments of the Benguela upwelling system. *Marine Geology* 163: 27–40.
- BRÜCHERT V., JØRGENSEN B.B., NEUMANN K., REICHMANN D., SCHLÖSSER M., and SCHULZ H. 2003. Regulation of bacterial sulfate reduction and hydrogen sulfide fluxes in the central Namibian coastal upwelling zone. *Geochimica Cosmochimica Acta* 67 (23): 4505–4518.
- BUCHAN S.H., CHALLINOR A., HARLAND W.B. and PARKER J.R. 1965. The Triassic stratigraphy of Svalbard. *Norsk Polarinstitute Skrifer* 135: 1–94.
- CALVERT S.E., THODE H.G., YEUNG D. and KARLIN R.E. 1996. A stable isotope study of pyrite formation in the Late Pleistocene and Holocene sediments of the Black Sea. *Geochimica Cosmochimica Acta* 60: 1261–1270.
- CANFIELD D.E. and THAMDRUP B. 1994. The production of <sup>34</sup>S-depleted sulfide during bacterial disproportionation of elemental sulphur. *Science* 266: 1973–1975.
- CANFIELD D.E., RAISWELL R., WESTRICH J.T., REAVES C.M. and BERNER R.A. 1986. The use of chromium reduction in the analysis of reduced inorganic sulphur in sediments and shales. *Chemical Geology* 54: 149–155.
- DALLMANN W.K. (ed.) 1999. Lithostratigraphic Lexicon of Svalbard. Upper Paleozoic to Quaternary Bedrock. Review and Recommendations for Nomenclature Use. Norsk Polarinstitutt, Tromsø: 318 pp.
- ESPITALIÉ J., DEROO G. and MARQUIS F. 1985. La pyrolyse Rock-Eval et ses applications. *Revue de l'Institut Français du Pétrole* 40: 563–579.
- FANLO I. and AYORA C. 1998. The evolution of the Lorraine evaporate basin: implications for the chemicals and isotope composition of the Triassic ocean. *Chemical Geology* 146: 135–154.
- FRITZ P., DRIMMIE R.J. and NOWICKI V.Y. 1974. Preparation of sulphur dioxide for mass spectrometer analyses by combustion of sulfides with copper oxide. *Analytical Chemistry* 46: 164–166.
- GAUTIER D.L. 1987. Isotopic composition of pyrite: Relationship to organic matter type and iron availability in some north American Cretaceous shales. *Chemical Geology* 65: 293–303.
- HABICHT K.S. and CANFIELD D.E. 1997. Sulphur isotope fractionation during bacterial sulfate reduction in organic-rich sediment. *Geochimica Cosmochimica Acta* 61: 5351–5361.
- HABICHT K.S., CANFIELD D.E. and RETHMEIER J. 1998. Sulphur isotope fractionation during bacterial reduction and disproportionation of thiosulfate and sulfite. *Geochimica Cosmochimica Acta* 62: 2585–2595.
- HURTGEN M.T., LYONS T.W., INGALL E.D. and CRUSE A.M. 1999. Anomalous enrichments of iron monosulfide in euxinic marine sediments and the role of H<sub>2</sub>S in iron sulfide transformations: Ex-

- amples from Effingham inlet, Orca Basin, and the Black Sea. *American Journal of Science* 229: 556–588.
- JØRGENSEN B.B. 1990. A thiosulfate shunt in the sulphur cycle in marine sediments. *Science* 249: 152–154.
- JØRGENSEN B.B., WEBER A. and ZOPFI J. 2001. Sulfate reduction and anaerobic methane oxidation in Black Sea sediments. *Deep-Sea Research I* 48: 2097–2120.
- JØRGENSEN B.B., BÖTTCHER M.E., LÜSCHEN H., NERETIN M.N. and VOLKOV I.I. 2004. Anaerobic methane oxidation and a deep H<sub>2</sub>S sink generate isotopically heavy sulfides in Black Seas sediments. *Geochimica Cosmochimica Acta* 68 (9): 2095–2118.
- KARCZ P. 2008. Genesis of Middle Triassic Spitsbergen black shales based on the geochemical indicators. Ph.D. Thesis. Institute of the Geological Sciences of the Polish Academy of Sciences. Warszawa: 161 pp.
- KARCZ P. 2009. Środowisko sedymentacji i wczesna diagenеза czarnych łupków ogniwa Passhatten (środkowy trias, Spitsbergen, Svalbard) na podstawie analizy geochemicznej. *Przegląd Geologiczny* 57 (10): 918–926.
- KRAJEWSKI K.P. 2000. Phosphogenic facies and processes in the Triassic of Svalbard. *Studia Geologica Polonica* 116: 7–84.
- KRAJEWSKI K.P., KARCZ P., WOŹNY E. and MØRK A. 2007. Type section of the Bravaisberget Formation (Middle Triassic) at Bravaisberget, western Nathorst Land, Spitsbergen, Svalbard. *Polish Polar Research* 28: 79–122.
- LEŚNIAK P.M., ŁĄCKA B., KRAJEWSKI P.K., ZAWIDZKI P. and HLADIKOWA J. 2003. Extreme sulphur isotopic fractionation between sulfate of carbonate fluoroapatite and authigenic pyrite in the Neocomian sequence at Wąwał, Central Poland. *Chemical Geology* 200: 325–337.
- LYONS T.W. 1997. Sulphur isotopic trends and pathways of iron sulfide formation in upper Holocene sediments of the anoxic Black Sea. *Geochimica Cosmochimica Acta* 61: 3367–3382.
- MØRK A. and BJØRØY M. 1984. Mesozoic source rock on Svalbard. In: A. M. Spencer *et al.* (eds) *Petroleum Geology of the North European Margin*. Norwegian Petroleum Society, Graham and Trotman, London: 371–382.
- MØRK A. and BROMLEY R.G. 2008. Ichnology of a marine regressive system tract: the Middle Triassic of Svalbard. *Polar Research* 27: 339–359.
- MØRK A., KNARUD R. and WORSLEY D. 1982. Depositional and diagenetic environments of the Triassic and Lower Jurassic succession of Svalbard. In: A.F. Embry and H.R. Balkwill (eds) *Arctic Geology and Geophysics. Canadian Society of Petroleum Geologist Memoir* 8: 371–398.
- MØRK A., EMBRY A.F. and WEITSCHAT W. 1989. Triassic transgressive-regressive cycles in the Sverdrup Basin, Svalbard and the Barents Shelf. In: J.D. Collinson (ed.) *Correlation in Hydrocarbon Exploration*. Graham and Trotman, London: 113–130.
- MØRK A., DALLMANN W.K., DYPWIK H., JOHANNESSEN E.P., LARSEN G.B., NAGY J., NØTTVEDT A., OLAUSSEN S., PČELINA T.M. and WORSLEY D. 1999. Mesozoic lithostratigraphy. In: W. K. Dallmann (ed.) *Lithostratigraphic Lexicon of Svalbard. Review and Recommendations for Nomenclature Use*. Upper Palaeozoic to Quaternary Bedrock. Norsk Polarinstitut, Tromsø: 127–214.
- NERETIN L.N., BÖTTCHER M.E., JØRGENSEN B.B., VOLKOV I.I., LÜSCHEN H. and HILGENFELDT K. 2004. Pyritization process and greigite formation in the advancing sulfidization front in the Upper Pleistocene sediments of the Black Sea. *Geochimica Cosmochimica Acta* 68 (9): 2081–2093.
- RIIS F., LUNDSCHIEN B.A., HØY T., MØRK A. and MØRK M.B.E. 2008. Evolution of Triassic shelf in the northern Barents Sea region. *Polar Research* 27: 318–338.
- STEEL R.J. and WORSLEY D. 1984. Svalbard's post Caledonian strata – an atlas of sedimentational patterns and paleogeographic evolution. In: A. M. Spencer *et al.* (eds) *Petroleum Geology of*

- the North European Margin*. Norwegian Petroleum Society. Graham and Trotman, London: 109–135.
- WEBER A., RIESS W., WENZHOEFER F. and JØRGENSEN B.B. 2001. Sulfate reduction in Black Sea sediments: in situ and laboratory radiotracer measurements from the shelf to 2000 m depth. *Deep-Sea Research I* 48: 2073–2096.
- WERNE J.P., LYONS T.W., HOLLANDER D.J., FORMOLO M.J. and DAMSTE J.S. 2003. Reduced sulphur in euxinic sediments of the Cariaco Basin: sulphur isotope constraints on organic sulphur formation. *Chemical Geology* 195: 159–179.
- ZABACK D. A. and PRATT L.M. 1992. Isotope composition and speciation of sulphur in the Miocene Monterey Formation: Reevaluation of sulphur reactions during early diagenesis in marine environments. *Geochimica Cosmochimica Acta* 56: 763–774.

Received 7 July 2009  
Accepted 9 September 2010